Efficient Wind Turbine Generation Planning for Decreasing Distribution System Company Payments in Real Applications

Mohammad Hasan Hemmatpour and Mohammad Hossein Rezaeian Koochi

***Abstract*—Wind energy has posed new challenges in both transmission and distribution systems owing to its uncertain nature. The effect of wind turbines (WTs) on the actual payments charged by upstream networks to distribution system companies (DISCOs) is one challenge. Moreover, when the grid-connected inverters of WT operate in the lead or lag modes, WTs absorb or inject reactive power from the system. This paper proposes an approach to assess the importance of operation modes of WTs to minimize the costs by DISCOs in the presence of system uncertainties. Accordingly, an optimization problem is formulated to minimize the costs to DISCO by determining the optimal locations and sizes of WTs in optimally reconfigured distribution systems. In addition, an improved vector-based swarm optimization (IVBSO) algorithm is proposed because it is highly suitable for vector-based problems. Two distribution systems are used in the simulations to evaluate the proposed algorithm. Firstly, the capabilities of the IVBSO algorithm to determine better solutions over other heuristic algorithms are confirmed using the IEEE 33-bus test system. Secondly, the Bijan-Abad distribution system (BDS) is used to demonstrate the effectiveness of the proposed optimization problem. Accordingly, the distribution system model, cumulative distribution function of wind speed, and load profile are all extracted from the actual data of the BijanAbad region. Finally, the optimization problem is applied to BDS in both the lead and lag modes of WTs. Results indicate that the total costs of DISCO are lower when WTs operate in the lag mode than in the lead mode.**

***Index Terms*—Distribution system companies (DISCOs), improved vector-based swarm optimization (IVBSO), reconfiguration, wind turbine, operation mode.**

I. Introduction

In recent decades, distributed generation (DG), including renewable and non-renewable power generation, has an increasing penetration in distribution systems. One of the most common sources of renewable energy is wind energy, which is converted to electricity using wind turbines (WTs). However, because wind speed is uncertain, the output energy generated by a WT is also uncertain. In addition, using WTs can decrease greenhouse gas emissions.

Numerous studies have been conducted in the field of renewable power generation. Hence, the effects of renewable energy sources on power system operation and planning are commonly studied, and new challenges are encountered by the utilities in different studies of microgrids [1] and distribution [2], and transmission systems [3]. For example, in [4], a next-generation of grid-connected renewable energy resources and load demand was proposed by considering the uncertainties in the system. A real-time economic dispatching considering the variability of renewable power generation and uncertainty of scheduling periods was presented in [5]. A market clearing mechanism was presented in [6], [7], and the effect of uncertainties on wind power generation was explicitly considered.

The reconfiguration of distribution systems and its role in increasing the reliability [8] and voltage stability [9] of distribution systems and microgrids [10] had study priorities in the last decade. In this context, different techniques with different purposes were proposed in the literature to investigate the role of reconfiguration and its effects. Moreover, another topic was the effect of DG penetration and reactive power compensators such as capacitors on the reconfiguration of distribution systems. For example, the effects of renewable energy sources, energy storage systems, demand response programs, and reconfiguration on the optimal sharing of energy were investigated in [11] and [12]. Considering the operation of the protection devices, the optimal simultaneous hourly reconfiguration and day-ahead scheduling framework were developed in smart distribution systems [13]. Other examples include the dynamic network reconfiguration for a time-varying load profile in the presence of DGs [14] and the multi-objective approach for network reconfiguration considering vehicle-to-grid with the integration of renewable energy [15]. Reference [16] proposed a method for reducing the costs of distribution system companies (DISCOs) in restructured networks with DGs using PV and PQ models. The frog leap algorithm was used as the solver and demonstrated that the net payment of DISCOs decreased in the presence of DGs. In [17], a genetic algorithm was used to solve the reconfiguration problem in the presence of DGs, considering that the bus voltage can be controlled by DGs. In [18], to-

Manuscript received: June 26, 2019; revised: September 3, 2019; accepted: March 23, 2020. Date of CrossCheck: March 23, 2020. Date of online publication: September 24, 2020.

M. H. Hemmatpour (corresponding author) is with the Electrical Engineering Department, Faculty of Engineering, Jahrom University, Jahrom, Iran (e-mail: m.h.hematpour@jahromu.ac.ir).

M. H. R. Koochi is with the Department of Electrical Engineering, Shahid Bahonar University of Kerman, Kerman, Iran (e-mail:mh_rezaeian@eng.uk.ac.ir).

DOI: 10.35833/MPCE.2019.000421

gether with optimal capacitor placement, a reconfiguration was performed to minimize the losses. In [19], the reconfiguration problem was solved in distribution systems considering different load levels and their effects on voltage stability.

DISCOs, which own and manage distribution systems economically and technically, encounter challenges such as decreasing electrical losses, balancing the load of feeders, and reducing the operation costs are crucial. Thus, the reconfiguration is the simplest and most cost-effective method to achieve these goals without adding extra equipments to the system. Note that although the installment of WTs imposes additional cost on DISCOs, the cost can be returned in a relatively short time due to the reduction in the payment of DISCOs by upstream utilities (if the WTs and their sizes are optimally determined). In addition to the optimal use of WTs, the time frame for the return rate can be further shortened if the distribution system is reconfigured. However, if the size of a WT is not selected appropriately, the initial goals of the problem cannot be achieved. Inappropriate selection can even cause severe problems in the system. For example, if the capacity of distribution lines is not sufficient to transmit the power generated by WTs, the phenomenon called wind power spillage occurs [20]. In some scenarios, the indices, i.e., the voltage stability index, will decrease by the increasing wind power ratio [21]. Therefore, it is essential to carefully evaluate the effects of wind power generation, particularly for actual scenarios.

In this paper, a new problem is defined to minimize the costs of DISCOs using the reconfiguration in the presence of WTs. The problem is formulated as a multi-objective problem, in which the operation constraints of the system are considered. When operating in the lead and lag modes, the effects of WTs are discussed, which make the results more practical, particularly in actual scenarios. An improved vector-based swarm optimization (IVBSO) is adopted to solve the optimization problem. Vectors with appropriate orientation gradually converge to a global optimum point, which is essential for vector-based optimization problems. The proposed algorithm is applied to two distribution systems. IEEE 33-bus system is used to demonstrate the effectiveness of the proposed algorithm by comparing the results with those of other studies. The proposed algorithm is then applied to an actual system (BijanAbad distribution system (BDS)), and the results are evaluated. In summary, the contributions of the proposed algorithm are summarized as follows.

1) A cost-oriented optimization problem is presented for distribution system planning considering the effects of WTs and the cost reconfiguration of DISCOs.

2) The operation modes of WTs are included to determine the best solutions for actual scenarios.

3) IVBSO algorithm is proposed as the optimization solver to minimize the costs to DISCO, owing to its unique capabilities for vector-based problems.

4) In addition to the standard test system, the efficiency of the proposed algorithm is evaluated using an actual distribution system.

II. Problem Formulation

In this paper, a multi-objective optimization problem is presented for decreasing the cost of DISCOs in electricity markets involving WTs. Three objective functions are included in the optimization problem, two of which are the cost functions corresponding to the active and reactive power consumed in a distribution system, and the other relates to the cost of installing a WT. In this paper, we aim to minimize the sum of the above three objective functions. Note that in a radial distribution system, the active power delivered from the upstream network equals to the sum of the active power consumed by loads and the active power losses, excluding the active power generated by WTs in the system. Thus, WTs may consume or generate the reactive power depending on their operation mode. If a WT operates in the lag mode, the reactive power consumption in the distribution system decreases due to the reactive power generated by the WT. If the WT operates in the lead mode, it consumes reactive power. Therefore, the total reactive power consumption increases. Three objective functions are discussed as follows.

A. Cost of Active Power

The first objective function F_1 is the cost of the active power injected from the upstream network:

$$F_1 = \lambda^p E^p = \lambda^p \left[\sum_{i=1}^{LL} \sum_{j=1}^{WSL} \left(P_{demand} + P_{loss} - P_{WT} \right) \rho_i^L \rho_j^W T \right] \quad (1)$$

where P_{demand}, P_{loss}, and P_{WT} are the active power demanded by all consumers, the active power losses, and the active power generated by WTs, respectively; ρ_i^L and ρ_j^W are the probabilities of the i^{th} load level and the j^{th} wind speed level, respectively; T is the time duration, which is considered to be 24 hours in this paper; λ^p is the cost of the active power per kWh; and LL and WSL are the numbers of load levels and wind speed levels, respectively. Note that the active power generated by a WT varies as a function of wind speed. As a result, WTs generate the power with a random value during a one-day time frame due to the stochastic nature of wind speed. Therefore, for a more accurate cost analysis of DISCOs, the stochastic nature of wind speed is also considered. Equation (2) shows the output power of a WT as a function of wind speed [21].

$$P_{WT}^i = \begin{cases} 0 & 0 < W_s^i < W_s^{ci}, W_s^i > W_s^{co} \\ P_r \dfrac{W_s^i - W_s^{ci}}{W_s^r - W_s^{ci}} & W_s^{ci} < W_s^i < W_s^r \\ P_r & W_s^r < W_s^i < W_s^{co} \end{cases} \quad (2)$$

where P_{WT}^i is the active power generated by the i^{th} WT; P_r is the rated power of WT; W_s^i is the wind speed at the place of the i^{th} turbine; W_s^{ci} and W_s^{co} are the cut-in and cut-out wind speeds of a WT, respectively; and W_s^r is the rated wind speed.

B. Cost of Reactive Power

The second objective function F_2 related to the cost of the reactive power flowing from the upstream network and is defined as:

$$F_2 = \lambda^q E^q = \lambda^q \left[\sum_{i=1}^{LL} \sum_{j=1}^{WSL} \left(Q_{demand} + Q_{loss} - Q_{WT} \right) \rho_i^L \rho_j^W T \right] \quad (3)$$

where Q_{demand}, Q_{loss}, and Q_{WT} are the reactive power demanded in the system, the reactive power losses, and the reactive power generated or consumed by WTs, respectively; and λ^q is the cost of reactive power per kWh.

C. Cost of Installing WT

The third objective function F_3 is the installation cost of WTs. According to [22], the installation cost of WTs with capacities ranging from 0.5 MW to 2.5 MW can be obtained:

$$F_3 = A_P + B_P P_{rated,WT} \quad (4)$$

where $P_{rated,WT}$ is the rated power of a WT; and A_P and B_P are two constants whose values are set to be –0.173 and 0.9966, respectively [22].

Finally, considering the above three objective functions, the final objective function is defined as the sum of F_1, F_2, and F_3 in (5), which is minimized using an analytical or heuristic method.

$$\min F_t = F_1 + F_2 + F_3 \quad (5)$$

D. Constraints of Proposed Approach

1) Power flow constraint

Power flow constraints are essential to guarantee the balance between generation and consumption in the system. These constraints are defined as:

$$\begin{cases} P_G(i) = P_D(i) + P_{loss}(i) \\ Q_G(i) = Q_D(i) + Q_{loss}(i) \end{cases} \quad (6)$$

where $P_G(i)$ and $Q_G(i)$ are the sums of the active power and reactive power injected by the upstream network and those generated by WTs in the distribution system at hour i, respectively; $P_D(i)$ and $Q_D(i)$ are the active power and the reactive power demanded by the consumers in the system, respectively; and $P_{loss}(i)$ and $Q_{loss}(i)$ are the active power and the reactive power losses at hour i, respectively.

2) Constraint related to bus voltage

The voltage of each bus i U_i maintains a value between the predefined minimum and maximum values, i.e.:

$$U_{i,\min} < U_i < U_{i,\max} \quad i = 1, 2, ..., N_{bus} \quad (7)$$

where $U_{i,\min}$ and $U_{i,\max}$ are the minimum and maximum boundaries of voltage at bus i, respectively; and N_{bus} is the number of the buses in the system.

3) Constraint related to line current

For each line i, the current flowing through the line $I_L(i)$ must not exceed the maximum allowable current value, i.e.:

$$I_L(i) \le I_{L,\max}(i) \quad i = 1, 2, ..., N_{br} \quad (8)$$

where $I_{L,\max}(i)$ is the maximum current value allowed to flow through the ith line due to thermal limit of the line; and N_{br} is the number of lines in the system.

4) Constraint related to radial structure of distribution system

Maintaining the radial structure of the distribution system is one of the important constraints that should be considered in system reconfiguration. Open breakers should be selected in a manner that the structure of the distribution system remains radial. In this paper, the Matroid method based on graph theory is used to ensure that the system remains radial after reconfiguration [10].

III. Proposed Algorithm for Solving Optimization Problem

IVBSO is an evolved version of the particle swarm optimization and the differential evolutionary algorithms, where the population explorer is characterized in the form of a vector [23]. In this paper, the IVBSO algorithm is used to maintain the reconfiguration in the presence of a large WT generation and load pattern variations. The main reason for using the IVBSO algorithm is that the vectors with appropriate orientations gradually converge to a global optimum point. Therefore, the IVBSO algorithm employs random coefficients with a proper strategy. The algorithm can be implemented through the following steps.

Step 1: formation of the initial population. The initial population vector contains the number of open switches representing the network configuration. Hence, the initial D-dimensional population vector, which contains N_{POP} number of members, is formed randomly based on the Matroid theory via the following equation:

$$V_{i,j}[0] = \begin{cases} randi & 1 \le i \le N_{Cap} \\ v_j^{low} + rand(0,1) \cdot \left(v_j^{up} - v_j^{low} \right) & N_{Cap} + 1 \le i \le N_{POP} \end{cases} \quad (9)$$

where $V_{i,j}[0]$ is the j^{th} dimension of the i^{th} initial population vector; i is the i^{th} population vector; $j \in [1, D]$ is the j^{th} dimension of the vector $\boldsymbol{V}_i$; $rand(0,1)$ is a function that generates a random number between 0 and 1; *randi* is a function for generating random integer values; v_j^{up} and v_j^{low} are the upper and lower limits of the j^{th} element of the corresponding vector, respectively; and N_{Cap} is the number of open switches in the distribution system.

Step 2: merit functions in vector optimization. In this step, the fitness of each vector is evaluated based on the objective function introduced in (5).

Step 3: population updating based on merit functions. Using the IVBSO algorithm, the new vectors are calculated through the following four stages: reproduction, mutation, boundary check, and selection.

1) Reproduction: this function combines several vectors to determine the best information and can be categorized into a direct cooperation vector $\boldsymbol{V}_{di,co}$, and differential cooperation vector $\boldsymbol{V}_{diff,co}$ to control the exploration and searches:

$$\boldsymbol{V}_{di,co}[k] = w_1 \boldsymbol{V}_{cu}[k] + w_2 \boldsymbol{V}_{ave}[k] + w_3 \boldsymbol{V}_{best}[k] + w_4 \boldsymbol{V}_{lb}[k] + w_5 \boldsymbol{V}_{rand}[k] \quad (10)$$

$$\boldsymbol{V}_{diff,co}[k] = w_6 \left(\boldsymbol{V}_{ave}[k] - \boldsymbol{V}_{cu}[k] \right) + w_7 \left(\boldsymbol{V}_{best}[k] - \boldsymbol{V}_{cu}[k] \right) + w_8 \left(\boldsymbol{V}_{lb}[k] - \boldsymbol{V}_{cu}[k] \right) + w_9 \left(\boldsymbol{V}_{rand}[k] - \boldsymbol{V}_{cu}[k] \right) \quad (11)$$

where $\boldsymbol{V}_{cu}$ is the current response vector; $\boldsymbol{V}_{ave}$ is the average response vector; $\boldsymbol{V}_{best}$ is the fittest response vector; $\boldsymbol{V}_{lb}$ is the best fittest vector within the neighboring of the i^{th} vector; $\boldsymbol{V}_{rand}$ is a random vector in each generation; and w_1 to w_9 are the coefficients. Note that $\boldsymbol{V}_{di,co}$ and $\boldsymbol{V}_{diff,co}$ are constructed

from a proper combination of vectors.

By adding $\boldsymbol{V}_{diff,co}$ to $\boldsymbol{V}_{di,co}$, the cooperation vector at stage k can be calculated as:

$$\boldsymbol{V}_{co}[k]=\boldsymbol{V}_{di,co}[k]+\boldsymbol{V}_{diff,co}[k] \tag{12}$$

The coefficients corresponding to the direct cooperation should be greater than those in the differential equation to prevent a solution from falling into a local optimum point. Therefore, w_1 to w_5 and w_6 to w_9 are selected with a probability of 50%, then, the following summations hold:

$$w_{D,C}=w_1+w_2+w_3+w_4+w_5\cong 1$$

$$w_{diff,c}=w_6+w_7+w_8+w_9\cong 0.5$$

If the coefficients are selected randomly with a uniform probability distribution, $w_{D,C}$ and $w_{diff,c}$ would also follow the random pattern with a uniform probability distribution. The coefficient w_i can be calculated using:

$$w_i=\frac{rand(0,2)}{n}=\frac{2rand(0,1)}{n}\quad i=1,2,...,5 \tag{13}$$

$$w_i=\frac{rand(0,1)}{n}\quad i=6,7,...,9 \tag{14}$$

where n is the number of non-zero coefficients in the direct and differential equations. It represents the number of cooperation vectors that are used in $\boldsymbol{V}_{diff,co}$ and $\boldsymbol{V}_{di,co}$.

2) Mutation: this operation is used to increase the diversity of solutions. The mutation equation can be defined using:

$$V_{mutation,i,j}[k]=\begin{cases}randi & 1\le i\le N_{Cap}\\ \dfrac{d}{100}\cdot rand\cdot\left(v_j^{up}-v_j^{low}\right) & N_{Cap}+1\le i\le N_{POP}\end{cases} \tag{15}$$

where d is a number that starts from 1 and dynamically decreases through the algorithm iterations to 0. Finally, the final updated vector will be calculated as:

$$\boldsymbol{V}[k]=\boldsymbol{V}_{co}[k]+\boldsymbol{V}_{mutation}[k] \tag{16}$$

where $\boldsymbol{V}[k]$ is the new solution vector called as offspring vector.

3) Boundary check: the boundary check is used to assure that the new solution vector confines within the range of the security constraints. Thus, if $V_{i,j}>v_j^{up}$, the value of $V_{i,j}$ can be constrained with the v_j^{up}, and if $V_{i,j}<v_j^{low}$, the value of $V_{i,j}$ is controlled by v_j^{low}.

4) Selection: among all the parent and children vectors, N_{Cap} will be selected based on the merit functions to form the next-generation population.

Step 4: termination condition. With a precision of 0.01, the solutions of the objective function in two consecutive iterations are the same. If the termination condition is not satisfied, this process will be iterated from *Step 2*.

Figures 1 and 2 show the flowchart of the IVBSO algorithm incorporated with the proposed algorithm to calculate the objective function defined in Section II. In addition, Fig. 3 shows the power flow algorithm to calculate the active and reactive power consumptions at each load and wind speed levels.

Active power losses for a system with b lines can be calculated as [9]:

$$P_{loss}=\sum_{l=1}^{b}R_lB_l^2 \tag{17}$$

where R_l and B_l are the resistance and current flowing through the l^{th} line, respectively. Equation (17) indicates that line currents are required for obtaining the active power losses.

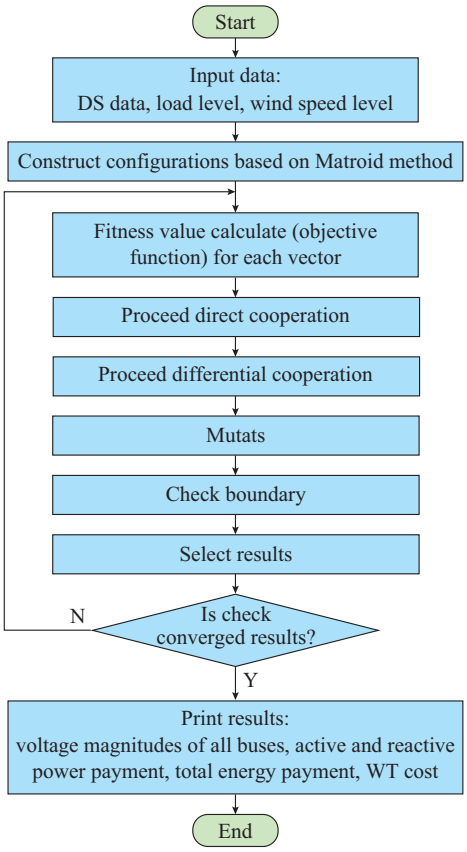

Fig. 1. Flowchart of IVBSO algorithm.

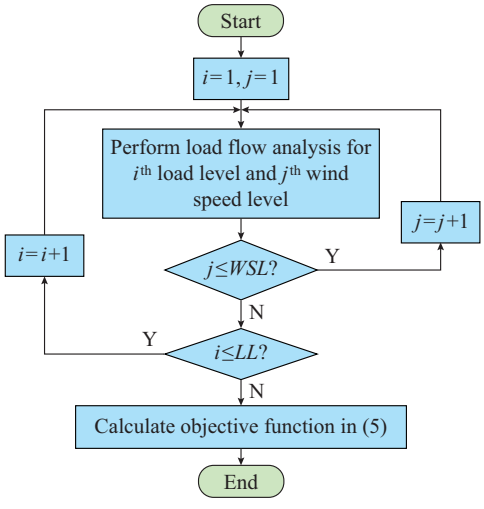

Fig. 2. Procedure for calculating objective function.

In this paper, they are calculated by applying distribution load flow (DLF) analysis [24], [25]. Different methods have been presented to date for load flow analysis in distribution systems, i.e., the backward-forward method, impedance ma-

trix calculation method, and DLF. In this paper, we aim to determine the best distribution system configuration, thus it is rapid and sufficiently necessary to apply a load flow method. The characteristics can be achieved by using DLF, in which the relationship between line currents and injected currents is presented by using the branch induction branch current (BIBC) matrix.

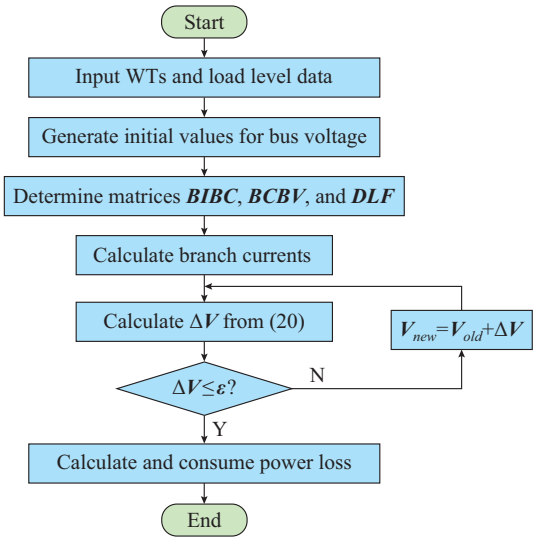

Fig. 3. Procedure of load flow analysis.

$$\boldsymbol{B} = \boldsymbol{BIBC} \cdot \boldsymbol{I} \tag{18}$$

where $\boldsymbol{B}$ and $\boldsymbol{I}$ are the matrices reflecting the current of the branches and buses of the system, respectively. The matrices interpreting the relationship between voltages and branch currents (BCBV) can be formed by initially using graph theory to determine the feeders in the system. Subsequently, voltage differences in the distribution system can be obtained by using the following equation:

$$\Delta \boldsymbol{V} = \boldsymbol{BCBV} \cdot \boldsymbol{B} \tag{19}$$

Equations (18) and (19) can be merged to achieve the relationship between the voltages of buses and the currents injected to buses:

$$\Delta \boldsymbol{V} = \boldsymbol{BCBV} \cdot \boldsymbol{I} \cdot \boldsymbol{BIBC} = \boldsymbol{DLF} \cdot \boldsymbol{I} \tag{20}$$

Equation (20) indicates that the magnitude and phase angle of voltages of all buses are required to calculate line currents. Therefore, according to [9], both voltage and current can be obtained by using an iterative procedure.

IV. Simulation Results

In this section, the proposed algorithm applying to two distribution systems is discussed. The first one is the IEEE 33-bus system and the second one is BDS, which is an actual system. Note that, for both systems, λ^p and λ^q are set to be 0.06 \$/kWh and 0.02 \$/kVAh, respectively [16].

A. Case Study 1: IEEE 33-bus System

IEEE 33-bus system is the first system to evaluate and demonstrate the effectiveness of the proposed algorithm over the existing methods. The IVBSO algorithm can be confirmed by using IEEE 33-bus system and comparing the results obtained for a simple reconfiguration problem with those of the previous studies. When more effective performance of the IVBSO algorithm is confirmed, it can be applied to the test system to solve the proposed optimization problem.

In this paper, a comparison is provided by simulating four scenarios for the IEEE 33-bus system as follows.

1) Scenario 1 (S1)

S1 is considered as the base case scenario without considering WTs. Figure 4 shows the single-line diagram of the IEEE 33-bus system. Under normal conditions, switches 33, 34, 35, 36, and 37 are open and the others are closed. The active power and reactive power in this system are 3715 kW and 2300 kvar, respectively [9]. In S1, the active and reactive power losses are 202.7 kW and 139.2 kvar, respectively. The voltage magnitudes of buses obtained from the power flow analysis are shown in Fig. 5. Because buses 18 and 33 are located at the end of their feeders, these buses are expected to have lowest amount of voltage.

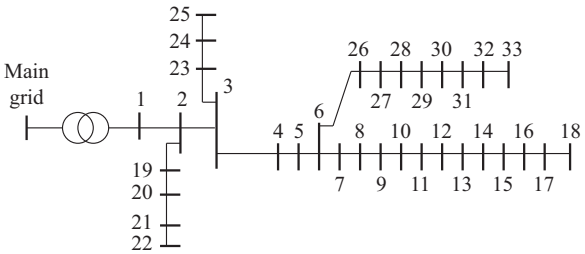

Fig. 4. Line diagram of IEEE 33-bus system.

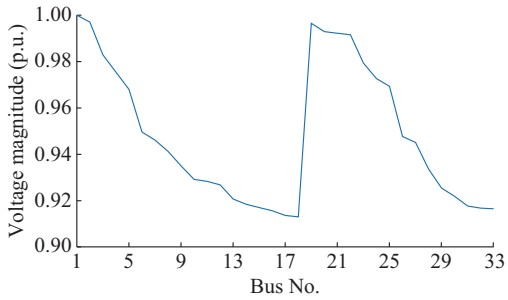

Fig. 5. Voltage profile of IEEE 33-bus system.

2) Scenario 2 (S2)

S2 is considered as the base case scenario considering WTs. The aim of S2 is to assess the effect of WTs with stochastic power generation on the base case results defined in S1. In S2, two WTs, each with a rated power of 500 kW, are assumed to be installed at buses with the minimum voltage, i.e. buses 18 and 33. Because this type of WT can operate in power factors with 0.9 leading or 0.9 lagging, power flow analysis is performed for both power factors and compared with that of S1. Load flow results are shown in Fig. 6. For WTs operating in the lag mode, the active and reactive power losses are 82.15 kW and 54.87 kvar, respectively. While for WTs operating in the lead mode, the active and reactive power losses are 166.28 kW and 139.2 kvar, respectively.

The comparison of the results with those in S1 indicates that installing WTs decreases the active and reactive power

losses regardless of the operation mode of WTs.

In S2, the voltage profile is also improved with WTs as shown in Fig. 6, which is primarily due to the decrease in the amount of power delivered from the upstream network and the direction change of the active power flow generated by WTs. For a better understanding of this challenge, consider the results in Fig. 6 and assume that WTs operate in the lag mode. The WT at bus 18 supplies the power demanded at buses 16, 17, and 18, which causes a decrease in system loss. Consequently, voltage profile is improved.

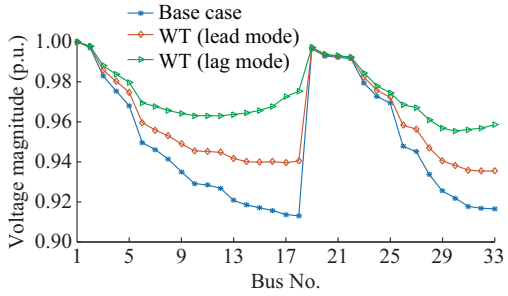

Fig. 6. Effect of WT operation modes on voltage profile.

3) Scenario 3 (S3)

S3 implements the system reconfiguration without considering WTs. It is defined to facilitate the evaluation effectiveness of the proposed optimization problem and compare it with other existing methods.

Minimizing the losses is considered as the main purpose of reconfiguration in literature. The reconfiguration for loss minimization is performed and a benchmark is provided to compare the performance of the proposed IVBSO algorithm with those of other algorithms. In S3, the proposed IVBSO algorithm is performed for 50 times and the dominant solution is selected as the optimum one.

The minimum losses obtained for IEEE 33-bus system is reported in [16]. Thus, the results of [16] are compared with those of S3, as shown in Table I. Figure 7 shows the convergence characteristic of the IVBSO algorithm in determining the best solution. Note that the values for each iteration shown in Fig. 7 are the differences between the two solutions obtained in two consecutive iterations.

TABLE I
COMPARISON OF RESULTS OF PROPOSED IVBSO ALGORITHM WITH LITERATURE

Algorithm	Power loss (kW)	No. of open switch
Proposed IVBSO	139.53	7, 9, 14, 32, 37
[19]	139.53	7, 9, 14, 32, 37

Table I indicates that the proposed algorithm produces the same results as those of [16], which has the best results in literature. One of the main reasons for the better performance of the proposed method over other methods is that it applied a restriction related to the radial structure of the system during the generation of the initial population. Consequently, the performance of the IVBSO algorithm is improved because non-feasible solutions (related to the configurations with non-radial topologies) are not generated in this manner. Therefore, the algorithm could search within the feasible solutions more effectively, prohibiting a shift to the local minimum.

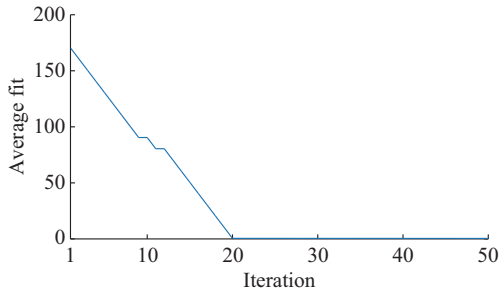

Fig. 7. Convergence characteristics of IVBSO algorithm in S3.

4) Scenario 4 (S4)

S4 implements the system reconfiguration with WTs, which covers the overall approach proposed in this paper. In S4, reconfiguration is performed considering different load levels and the probabilities of different wind speeds. The probabilities of the load levels and wind speeds are shown in Tables II and III, respectively [22]. The active power generated by a WT with respect to the wind speed can be calculated using (2). In this paper, the rated, cut-in, and cut-out wind speeds are assumed to be 10, 3, and 15 m/s, respectively.

TABLE II
LOAD LEVELS AND THEIR PROBABILITIES USED FOR IEEE 33-BUS SYSTEM

Probability	Wind speed limit (m/s)	Probability	Wind speed limit (m/s)
0.089	9-10	0.073	0-4
0.109	10-11	0.024	4-5
0.101	11-12	0.032	5-6
0.109	12-13	0.044	6-7
0.062	13-14	0.046	7-8
0.236	14-15	0.075	8-9

TABLE III
WIND SPEED LEVELS AND THEIR CORRESPONDING PROBABILITIES USED FOR IEEE 33-BUS SYSTEM

Percentage of peak load (%)	Probability	Percentage of peak load (%)	Probability
100.0	0.0010	58.5	0.1630
85.3	0.0560	51.0	0.1630
77.4	0.1057	45.1	0.0920
71.3	0.1654	40.6	0.0473
65.0	0.1654	35.1	0.0330

In the procedure of the proposed IVBSO algorithm, the initial values are set according to the results of S3. Moreover, the objective function used in S3 is the one defined in (5). The results of S4 are detailed in Table IV, including the two operation modes considered for WTs.

TABLE IV
COMPARISON OF RESULTS OBTAINED IN S4 WITH THOSE OF BASE CASE

Scenario	No. of open switch	E^p (kW)	E^q (kvar)	Total energy payment ($)	WT cost (M$)
Base case (load mode)	33, 34, 35, 36, 37	4864.8	3244.3	6861.8	
S4 (lag mode)	6, 9, 14, 32, 37	426.0	1261.5	3926.0	0.99642
S4 (lead mode)	7, 11, 14, 17, 37	410.6	377.7	3657.8	0.99642

Table IV indicates that, by installing WTs and performing reconfiguration, the total costs decrease by 46.69% and 42.78% when the WTs operate in the lag and lead modes, respectively. Moreover, the rated power of WTs (1000 kW) is 29.17% of the total active power in IEEE 33-bus system. A considerable share of active power demanded in the system is supplied by the WTs during 24 hours. It leads to the total cost reduction.

Figure 8 shows the voltage profile of the test system for the three scenarios, i.e., S1, S4 when WTs operating in the lag mode, and S4 when WTs operating in the lead mode. The convergence performance of the proposed IVBSO algorithm for S4 is shown in Figs. 9 and 10 for both modes.

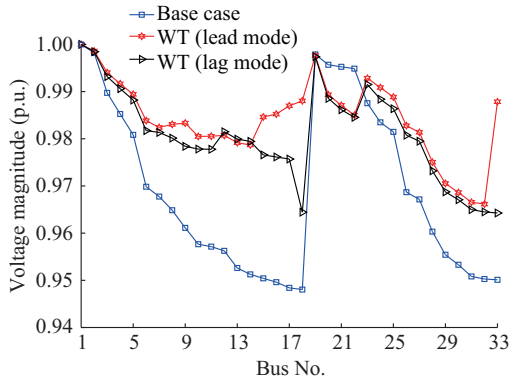

Fig. 8. Voltage profile corresponding to scenarios in Table IV.

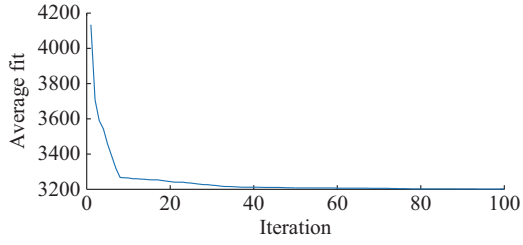

Fig. 9. Convergence performance of proposed IVBSO algorithm to optimal solution in S4 (lag mode).

Along with the results shown in Table IV, the voltage profile in Fig. 8 demonstrates the effectiveness of the proposed algorithm in determining a better solution. Generally, these results indicate that the best solution relates to the situation when WTs operate in the lag mode. The reason is that the operation costs decrease in a 24-hour time frame due to the significant reduction in active and reactive power consumptions.

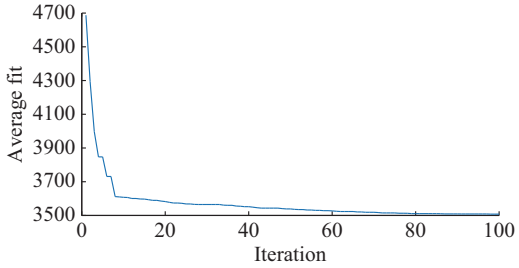

Fig. 10. Convergence performance of proposed IVBSO algorithm to optimal solution in S4 (lead mode).

B. Case Study 2: BDS

BDS is used to evaluate the performance of the proposed algorithm in actual applications. BDS is a large-scale, 75.3-km distribution system with 213 buses, and its demand is 7878.8 kW and 3815.9 kvar under normal loading conditions. The line diagram of this system is shown in Fig. 11. Note that the locations of only a few buses are shown in this figure. The details of the bus connections in BDS are provided in Table AI of Appendix A [26], where T denotes "to bus" and F denotes "from bus".

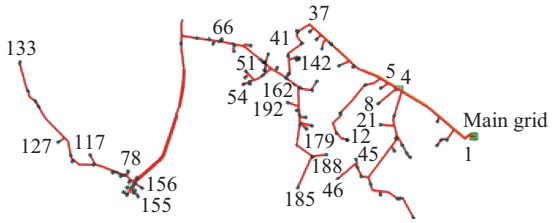

Fig. 11. Line diagram of BDS.

A geographic information system (GIS) is used to extract the required data. The geographical and technical data of the equipment are accessed, including the type data of lines and cables, configuration data, and data related to transformers and switches. These data can be input into MATLAB.

Different load levels of BDS are detailed in Table V [26], which indicates that the highest loading in BDS is 1.25 times higher than the normal loading, whereas the lowest loading value is 0.6. Moreover, according to this table, BDS is overloaded with the probability of 9.8%, which means that the system has experienced overloading.

TABLE V
LOAD LEVELS AND THEIR PROBABILITIES IN BDS

Percentage of peak load (%)	Probability	Percentage of peak load (%)	Probability
125.0	0.020	88.9	0.181
117.0	0.036	81.7	0.123
110.0	0.042	74.4	0.083
100.0	0.171	67.2	0.152
96.1	0.151	60.0	0.042

The load flow results for the heavy (125%), light (60%), and normal load levels (100%) of BDS are shown in Table VI. In addition, the voltage profile of the system is shown in Fig. 12. Note that there is no WT in the above three load

flow analyses. The difference of voltage phase angle between two incident buses is high. Therefore, the reactive power loss is higher than the active power loss in this system. These conditions can also be proven by the fact that a considerable share of total load in BDS is related to agricultural loads with high reactive power consumption.

TABLE VI
POWER LOSS AT VARIOUS LOAD LEVELS IN BDS

Loading state	Active power loss (kW)	Reactive power loss (kvar)
Light	105.52	106.53
Normal	292.96	295.76
Heavy	457.61	461.96

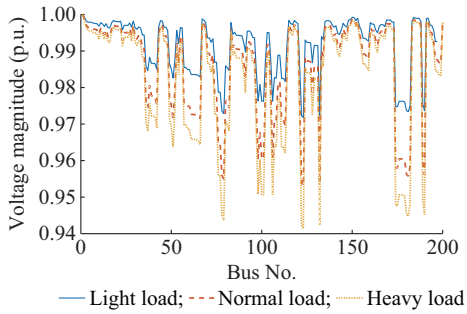

Fig. 12. Network voltage profile in BDS at various load levels.

The effects of WTs on BDS are included by inputting wind data to the problem. The data related to the wind speeds at the BijanAbad region are adopted from [27]. The time frame is from June 28, 2006 to July 1, 2008, and the data are measured every 10 min. Since the amount of wind speed data are extremely large, a maximum-likelihood estimator is used to determine the probability distribution function which is best fit for the wind speed data [28]. The Weibull distribution with parameters defined in (21) and (22) is observed to be best fit for the wind speed data.

$$f(v,k,c)=\left(\frac{k}{c}\right)\left(\frac{v}{c}\right)^{k-1}\exp\left(-\left(\frac{v}{c}\right)^{k}\right) \tag{21}$$

$$F(v,k,c)=1-\exp\left(-\left(\frac{v}{c}\right)^{k}\right) \tag{22}$$

In the above Weibull distribution, the values of c and k obtained for the wind speed function in BDS are 4.004 and 1.69, respectively. Figure 13 shows the probability density function of the wind speed for BDS.

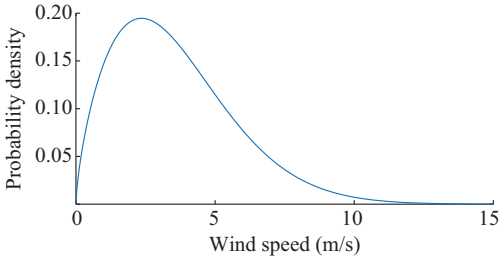

Fig. 13. Wind probability density function for BDS.

According to the probability distribution function shown in Fig. 13, twelve levels are considered for wind speeds as shown in Table VII. Considering various load levels of BDS as shown in Table V, the total payment of DISCO in the base case during 24 hours is $12002.03, which is shown in Table VIII. In addition, Table VIII shows the optimum locations and capacities of WTs and the optimum configuration of BDS, considering different load and wind speed levels in both lead and lag modes. In addition, the profits obtained from installing WTs in BDS during 24 hours in the lead and lag modes are $135.4 and $217.55, respectively. The cost of WTs is calculated as $996420, and the investment return rate when the WTs operate in the lead and lag modes would be 242 and 151 months, respectively. However, other benefits of installing WTs, i. e., the compatibility with the environment and the reduction of CO_2 emissions, are not considered in this paper.

TABLE VII
WIND SPEED LEVELS AND CORRESPONDING PROBABILITIES IN BDS

Probability	Wind speed limit (m/s)	Probability	Wind speed limit (m/s)
0.061	6-7	0.091	0-1
0.036	7-8	0.177	1-2
0.020	8-9	0.194	2-3
0.010	9-10	0.173	3-4
0.005	10-13	0.135	4-5
0.003	13-15	0.095	5-6

TABLE VIII
RESULTS OF PROPOSED METHODOLOGY FOR BDS

Scenario	Open switches on WTs	E^p (kW)	E^q (kvar)	Total energy payment ($)	WT cost (M$)
Base case (load level)	238, 239 (-)	4832.8	2396.1	12002.03	
WTs (lag mode)	61, 73 (5, 54)	4781.5	2367.6	11866.63	0.99642
WTs (lead mode)	61, 71 (5, 51)	4748.7	2351.3	11784.48	0.99642

V. CONCLUSION

In addition to the environmental benefits of using WTs for power generation, technical benefits can be achieved if WTs are allocated optimally. The technical benefits can be further augmented if the reconfiguration is applied to the system, leading to more economic benefits for DISCO. In this paper, an optimization problem is proposed to minimize the costs to DISCOs considering the operation effects of WTs on the distribution system. The IVBSO algorithm is proposed as the solver because it is highly suitable for vector-based optimization problems. To evaluate the proposed optimization problem, an IEEE 33-bus test system and BDS are used in the simulations. The results indicate that by determining the optimal configuration of the system and the optimal locations and sizes of WTs, DISCOs can achieve the least costs when WTs are operated in the lag mode. The results prove that, al-

though the installation cost of WTs is high for DISCOs, it can be returned in a short period if the reconfiguration is applied and WTs are operated in the lag mode. If WTs are operated in the lead mode, the investment return rate would be 1.6 times higher than the investment rate obtained when WTs are operated in the lag mode. With more installed WTs for the normal load, the investment return rate will be high. If the power generated by WTs can be transmitted in the system, the return rate can be improved by installing WTs with higher capacities. Therefore, the planning of applying WTs with high capacities is limited by operation constraints. However, considering the results obtained in this paper, future studies can be conducted as follows:

1) Demand response programs and their effects on the location of WTs can be considered.

2) PV power stations can be considered with probabilistic output as another type of power generation solely or with WTs.

APPENDIX A

TABLE AI
DETAILS OF BUS CONNECTIONS IN BDS

F	T	F	T	F	T	F	T	F	T	F	T	F	T	F	T	F	T	F	T
1	2	44	45	87	88	130	131	173	174	17	23	64	66	108	109	150	152	165	195
2	3	44	46	87	89	130	132	173	175	16	24	66	67	109	110	149	153	164	196
2	4	43	47	89	90	123	133	175	176	13	25	67	68	109	111	148	154	159	197
4	5	47	48	89	91	72	134	176	177	25	26	68	69	108	112	147	155	197	198
5	6	47	49	91	92	71	135	176	178	25	27	69	70	112	113	144	156	197	199
5	7	42	50	92	93	70	136	178	179	10	28	70	71	112	114	143	157	199	200
5	8	37	51	93	94	69	137	178	180	28	29	71	72	91	115	157	158	200	201
4	9	51	52	93	95	137	138	175	181	29	30	72	73	84	116	157	159	200	202
9	10	52	53	92	96	137	139	181	182	29	31	73	74	83	117	159	160	199	203
10	11	53	54	96	97	139	140	182	183	31	32	73	75	117	118	160	161	203	204
11	12	54	55	96	98	140	141	183	184	32	33	75	76	118	119	160	162	203	205
11	13	54	56	98	99	141	142	184	185	32	34	75	77	118	120	162	163	140	206
13	14	53	57	99	100	141	143	184	186	31	35	77	78	117	121	162	164	139	207
14	15	52	58	99	101	143	144	186	187	35	36	77	79	82	122	164	165	68	208
14	16	58	59	101	102	144	145	186	188	35	37	79	80	79	123	165	166	67	209
16	17	58	60	102	103	145	146	183	189	37	38	80	81	123	124	166	167	66	210
17	18	60	61	103	104	145	147	182	190	38	39	80	82	124	125	166	168	51	211
18	19	60	62	103	105	147	148	181	191	38	40	82	83	124	126	168	169	28	212
18	20	62	63	102	106	148	149	170	192	40	41	83	84	126	127	169	170	9	213
20	21	62	64	101	107	149	150	169	193	40	42	84	85	126	128	170	171	49	55
20	22	64	65	98	108	150	151	168	194	42	43	85	86	128	129	171	172	55	129

REFERENCES

[1] M. H. Hemmatpour, M. Mohammadian, and A. A. Gharaveisi, "Simple and efficient method for steady-state voltage stability analysis of islanded microgrids with considering wind turbine generation and frequency deviation," *IET Generation, Transmission & Distribution*, vol. 10, no. 7, pp. 1691-1702, May 2016.

[2] A. Karimi, F. Aminifar, A. Fereidunian *et al*., "Energy storage allocation in wind integrated distribution networks: an MILP-Based approach," *Renewable Energy*, vol. 134, pp. 1042-1055, Apr. 2019.

[3] M. H. Hemmatpour, E. Zarei, and M. Mohammadian, "Incorporating wind power generation and demand response into security-constrained unit commitment," *AUT Journal of Electrical Engineering*, vol. 50, no. 2, pp. 141-148, Sept. 2018.

[4] S. S. Reddy, "Optimization of renewable energy resources in hybrid energy systems," *Journal of Green Engineering*, vol. 7, no. 1, pp. 43-60, Jan. 2017.

[5] S. S. Reddy, P. Bijwe, and A. R. Abhyankar, "Real-time economic dispatch considering renewable power generation variability and uncertainty over scheduling period," *IEEE Systems Journal*, vol. 9, no. 4, pp. 1440-1451, Jun. 2014.

[6] S. S. Reddy, P. Bijwe, and A. Abhyankar, "Optimum day-ahead clearing of energy and reserve markets with wind power generation using anticipated real-time adjustment costs," *International Journal of Electrical Power & Energy Systems*, vol. 71, pp. 242-253, Oct. 2015.

[7] S. S. Reddy, P. Bijwe, and A. R. Abhyankar, "Optimal posturing in day-ahead market clearing for uncertainties considering anticipated real-time adjustment costs," *IEEE Systems Journal*, vol. 9, no. 1, pp. 177-190, Jun. 2013.

[8] I. Sarantakos, D. M. Greenwood, J. Yi *et al*., "A method to include component condition and substation reliability into distribution system reconfiguration," *International Journal of Electrical Power & Energy Systems*, vol. 109, pp. 122-138, Jul. 2019.

[9] M. H. Hemmatpour, M. Mohammadian, and M. R. Estabragh, "A novel approach for the reconfiguration of distribution systems considering the voltage stability margin," *Turkish Journal of Electrical Engineering & Computer Sciences*, vol. 21, pp. 679-698, May 2013.

[10] M. H. Hemmatpour, M. Mohammadian, and A. A. Gharaveisi, "Optimum islanded microgrid reconfiguration based on maximization of system loadability and minimization of power losses," *International Journal of Electrical Power & Energy Systems*, vol. 78, pp. 343-355, Jun. 2016.

[11] E. Hooshmand and A. Rabiee, "Energy management in distribution systems, considering the impact of reconfiguration, RESs, ESSs and DR: a trade-off between cost and reliability," *Renewable Energy*, vol. 139, pp. 346-358, Aug. 2019.

[12] S. F. Santos, D. Z. Fitiwi, M. R. M. Cruz *et al*., "Impacts of optimal energy storage deployment and network reconfiguration on renewable integration level in distribution systems," *Applied Energy*, vol. 185, pp. 44-55, Jan. 2017.

[13] S. Esmaeili, A. Anvari-Moghaddam, S. Jadid *et al*., "Optimal simultaneous day-ahead scheduling and hourly reconfiguration of distribution systems considering responsive loads," *International Journal of Electrical Power & Energy Systems*, vol. 104, pp. 537-548, Jan. 2019.
[14] A. Azizivahed, H. Narimani, M. Fathi *et al*., "Multi-objective dynamic distribution feeder reconfiguration in automated distribution systems," *Energy*, vol. 147, pp. 896-914, Mar. 2018.
[15] S. Cheng and Z. Li, "Multi-objective network reconfiguration considering V2G of electric vehicles in distribution system with renewable energy," *Energy Procedia*, vol. 158, pp. 278-283, Feb. 2019.
[16] B. Arandian, R.-A. Hooshmand, and E. Gholipour, "Decreasing activity cost of a distribution system company by reconfiguration and power generation control of DGs based on shuffled frog leaping algorithm," *International Journal of Electrical Power & Energy Systems*, vol. 61, pp. 48-55, Oct. 2014.
[17] S. Das, D. Das, and A. Patra, "Reconfiguration of distribution networks with optimal placement of distributed generations in the presence of remote voltage controlled bus," *Renewable and Sustainable Energy Reviews*, vol. 73, pp. 772-781, Jun. 2017.
[18] S. Sultana and P. K. Roy, "Oppositional krill herd algorithm for optimal location of capacitor with reconfiguration in radial distribution system," *International Journal of Electrical Power & Energy Systems*, vol. 74, pp. 78-90, Jan. 2016.
[19] M. H. Hemmatpour and M. Mohammadian, "An evolutionary approach for optimum reconfiguration and distributed generation planning considering variable load pattern based on voltage security margin," *Arabian Journal for Science & Engineering (Springer Science & Business Media BV)*, vol. 38, no. 12, pp. 3407-3420, Aug. 2013.
[20] M. Eslaminia, M. Mohammadian, and M. H. Hemmatpour, "An approach for increasing wind power penetration in deregulated power system," *Scientia Iranica*, vol. 23, no. 3, pp. 1282-1293, Dec. 2016.
[21] M. H. Hemmatpour, "Optimum interconnected islanded microgrids operation with high levels of renewable energy," *Smart Science*, vol. 7, no. 1, pp. 47-58, Nov. 2019.
[22] S. Lundberg, "Performance comparison of wind park configurations," Chalmers University of Technology, Goteborg, Sweden, Tech. Rep. 30 R, Aug. 2003.
[23] A. Afroomand and S. Tavakoli, "Vector-based swarm optimization algorithm," *Applied Soft Computing*, vol. 37, pp. 911-922, Dec. 2015.
[24] J. Teng and C. Chang, "A novel and fast three-phase load flow for unbalanced radial distribution systems," *IEEE Transactions on Power Systems*, vol. 17, no. 4, pp. 1238-1244, Nov. 2002.
[25] J. H. Teng, "A network-topology-based three-phase load flow for distribution system," *Source: Proceedings of the National Science Council, Republic of China, Part A: Physical Science and Engineering,* vol. 24, no. 4, pp. 259-264, Jul. 2000.
[26] Management of Generation, Transmission and Distribution of Electric Power in Iran (Tavanir). (2018, Jan.). [Online]. Available: http://www.tavanir.org.ir/
[27] Renewable Energy and Energy Efficiency Organization (SATBA). (2010, Jun.). [Online]. Available: http://www.satba.gov.ir/
[28] O. Alavi, A. Sedaghat, and A. Mostafaeipour, "Sensitivity analysis of different wind speed distribution models with actual and truncated wind data: a case study for Kerman, Iran," *Energy Conversion and Management*, vol. 120, pp. 51-61, Jul. 2016.

Mohammad Hasan Hemmatpour received the B.S., M.S., and Ph.D. degrees in electrical engineering from the Shahid Bahonar University of Kerman, Kerman, Iran, as an honor student in 2009, 2012, and 2016, respectively. Currently, he is an Assistant Professor at the Electrical Engineering Department of Jahrom University, Jahrom, Iran. His research interests include operation, controls and analysis of microgrids and distribution system, optimization techniques, and renewable energy modeling.

Mohammad Hossein Rezaeian Koochi received the B.S. degree in electrical engineering from Shahid Bahonar University of Kerman, Kerman, Iran, in 2010, the M.S. degree in electrical engineering from Iran University of Science and Technology (IUST), Tehran, Iran, in 2012, and the Ph.D. degree in electrical engineering from Shahid Bahonar University of Kerman, Kerman, Iran, in 2017. In 2016, he was a Visiting Research Scholar at the Queensland University of Technology, Brisbane, Australia. His research interests include energy management systems, smart grids, wide area measurement and control systems, power system dynamics and control, and pattern recognition and data mining in power systems.